

## **STUDY OF THE INFLUENCE OF COILING-UNCOILING INDUCED RESIDUAL STRESSES ON THE FATIGUE BEHAVIOR OF TRUCK FRAME RAIL SECTIONS**

CHINNARAJ K.<sup>1</sup>, SATHYA PRASAD M.<sup>1</sup>,  
LAKSHMANA RAO C.<sup>2</sup>, PADMANABAN R.<sup>3,\*</sup>

<sup>1</sup>Ashok Leyland Technical Centre, Chennai, India

<sup>2</sup>Indian Institute of Technology Madras, India

<sup>3</sup>Department of Mechanical Engineering, Amrita School of Engineering, Coimbatore,  
Amrita Vishwa Vidyapeetham, Amrita University, India

\*Corresponding Author: dr\_padmanaban@cb.amrita.edu

### **Abstract**

Coiling of steel sheet is one of the easiest methods adopted by steel mills for the compact transportation of bulk sheet material to truck manufacturers for making 'C' shaped side frame rails. The coiling-uncoiling operation induces residual stresses in the steel sheet due to plastic strain hardening. This initial imperfection in the form of residual stresses remains in the plain web and flange areas of the rail sections. In corner areas of frames, increase in residual stresses are observed due to severe plastic deformation from forming operation than the coiling-uncoiling operation. More accurate consideration of the residual stresses becomes necessary when the behaviour of truck side frame rail web and flange sections, derived from different coil diameters are assessed. In this work, micro-hardness measurement is employed to predict the extent of plastic deformation at different coil diameter locations. The residual stresses induced by the coiling-uncoiling operation is assessed using the X-ray diffraction technique for steel coil diameters ranging from 600 mm to 1800 mm. Fatigue tests on samples extracted from different coil diameters indicate that fatigue life increases with the increase in coil diameter of the sample. The fatigue life of the annealed flat test sample was found to be higher than the fatigue life of samples derived from different coil diameter locations of steel coils received from steel mills.

Keywords: Coiling-uncoiling, Fatigue life, Residual stress, Strain hardening.

## 1. Introduction

Demand for lightweight design of road vehicles in addition to rigorous regulatory norms has impelled the automotive designer's to explore intricate design details in order to achieve light weighting, cost reduction and improving the durability of components. Advances in finite element simulation and availability of high-speed computing resources have enabled simulations during the design stage itself, aiding and exploring the designer's concepts. The customary approach of using virgin material properties in the analysis of the structural behaviour of truck frame rails would not reflect its actual behaviour. Various stages of frame manufacturing operations such as a coiling-uncoiling roll or press forming and shot-peening are involved to achieve the final shape of truck frame rail sections. Each of these operations induces some amount of residual stress, influencing the behaviour of frame rail sections. Hence, the magnitude and direction of these stresses should be accounted for precisely.

Quach, et al. [1-4] have proposed an analytical solution for the residual stresses and co-existent equivalent plastic strains in stainless steel sections. They have observed that the coiling-uncoiling process induce residual stresses in the flat areas of a press-braked section while the residual stresses in corner areas are mainly due to cold forming operation. Moen, et al. [5] presented a mechanics-based method for determining the initial state of cold-formed steel members subject to coiling and cross-section roll forming for use in subsequent analysis. Cruise and Gardner [6] have discussed the residual stress variations along with the thickness in stainless steel sections and experimentally quantified the same due to three different production routes namely hot rolling, press braking and cold rolling.

Chinnaraj et al. [7-9] in their previous works suggest the need for accounting the effect of residual stress in cold-formed truck frame sections while analysing its structural behaviour. X-ray diffraction measurement method along with a new spot layer removal method was used to quantify the residual stresses in the thickness direction for both web and corner areas of press-formed truck frame sections. In this paper, the effect of through-thickness residual stresses resulting from the coiling-uncoiling operation on the overall frame fatigue behaviour is investigated by conducting fatigue life experiments.

## 2. Frame Rail and Material Properties

The steel coil and the 'C' shaped truck frame rail formed from the steel sheet drawn from the coil are shown in Figs. 1(a) and (b) respectively.

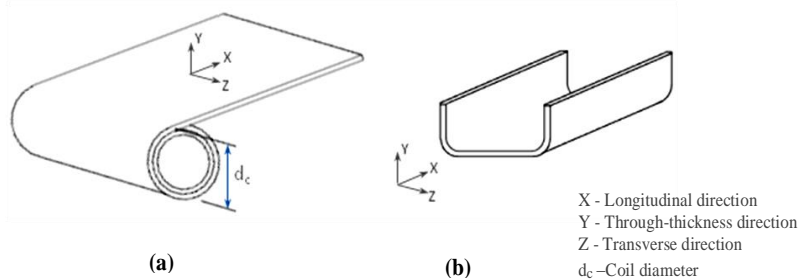


**Fig. 1(a) Steel coil sheet, (b) derived 'C' shaped truck frame rail sample.**

In this study, the material chosen for the rails is most widely used high strength low-alloyed steel BSK46, produced by controlled cooling after hot rolling. The chemical composition of the steel is given in Table 1.

The mechanical properties of the material namely Elastic modulus, Yield strength and Poisson ratio are 210 GPa, 460 MPa and 0.29 respectively. The mechanical properties of the material in terms of stress-strain characteristics are depicted in Fig. 2.

**Table 1. Composition of BSK46 steel material.**

Alloying elements	C	Mn	Nb	Si	P	S	Fe
Wt%	1.4	0.03	0.05	0.03	0.03	0.1	Bal.

### 3. Experimental Measurement method

The micro-hardness, residual stress and fatigue life of steel sheets at different coil diameter locations were measured experimentally as discussed in the following sections.

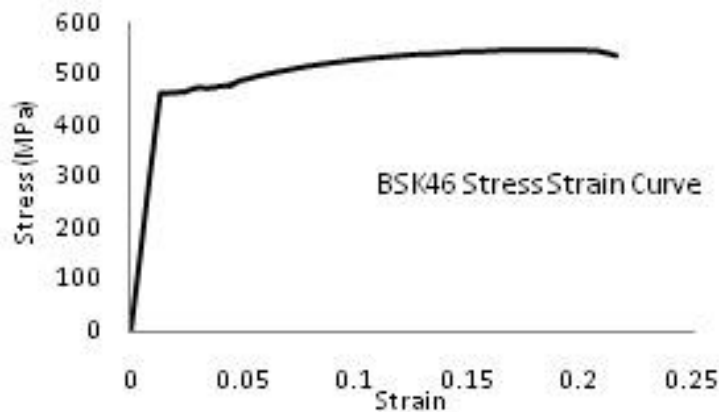


**Fig. 2. BSK46 Alloy carbon steel stress-strain characteristics.**

#### 3.1. Micro-hardness measurement

In order to quantify the through-thickness residual stresses remaining in the steel sheets at different coil diameter locations more accurately, the extent of through-thickness plastic deformation due to coiling-uncoiling operation is first assessed with the aid of micro-hardness measurement. In this work, the micro-hardness measurements were made using Vickers Hardness tester at different sheet thicknesses of steel specimens extracted from various coil diameter locations.

#### 3.2. Residual stress measurement

The residual stresses at different thicknesses of steel coil samples were measured using the X-ray diffractometer (Rigaku make) shown in Fig. 3. Chromium radiation is used by the diffractometer to obtain the diffraction peaks and the  $2\theta$  angle of the instrument is  $156^\circ$ . The  $\text{Sin } 2\psi$  technique was utilised with the lattice strain measured for different  $\psi$  angle tilts of the specimen. The residual stress at the

surface then arrives from the slope of best-fit least-squares straight line for the lattice strain as a function of  $\sin 2\psi$ . The method employed and the measurements done in both transverse and longitudinal directions of flat web sections at various thickness depths are presented in the following section.



(Courtesy: Central XRD Lab, IIT Madras, India).

**Fig. 3. Residual stress measurement setup.**

### 3.3. Spot layer removal method

Since X-ray Diffraction Technique (XRD) can be employed only for the measurement of the surface residual stress of any component, measurement of through-thickness residual stresses was accomplished here with the help of material removal as layers to the required depths. In standard layer removal method, the material on the surface is removed by rough machining of the entire surface followed by electrolytic polishing at the end [10]. In this study, material removal to required depths on the selected spot of a specimen is achieved by an electrolytic etching process using the setup shown in Fig. 4. Insulation tape is used for masking the test specimen almost completely, except a small area of  $1\text{ cm}^2$  size from where material removal is effected by exposing it to the electrolyte during the process.

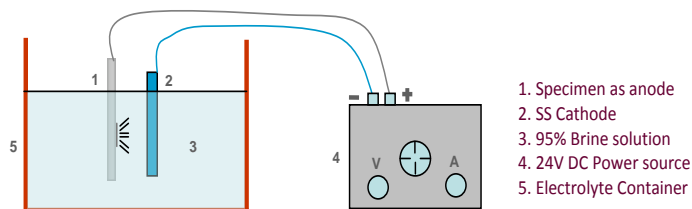


**Fig. 4. Set-up for electrolytic etching process.**

The electrolyte used is 95% brine solution and the material surface is exposed to the electrolyte for a pre-set time period for material removal to the required depth. During this process, the electrolyte temperature is to be maintained constant to avoid any thermal induced effect on the specimen. XRD measurement of residual stress over the tiny area becomes difficult as the depth increases. Therefore, residual stresses in one-half thickness of the specimen are measured from the outside

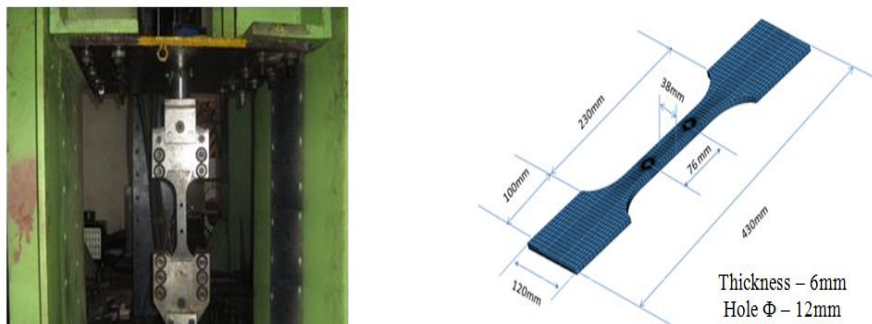
surface, while the residual stresses in the remaining half thickness of the specimen are measured from the inside surface at the same location.

The benefit of using the electrolytic etching process is that the initial machining of the surface is eliminated. Due to this, residual stresses due to rough machining are not introduced into the component subsurface. In addition, as the removal of material is effected on a small selected local area residual stress relaxation is also very less.

### 3.4. Fatigue life experiments

To assess the influence of the coiling-uncoiling residual stresses on the fatigue life of the frame, fatigue samples with specification as shown in Fig. 5 were tested using a 100 kN fatigue testing machine (servo-hydraulic).

For this, the test sample materials extracted from different coil diameter locations and an annealed flat steel sheet as received from steel mill before coiling are arranged as one stack and cut using water jet cutting in one stroke. This will ensure that the section profiles had uniform cutting parameters and their fatigue performance is free from the influence of the cutting process.



(Courtesy: Ashok Leyland Technical Centre, India).

**Fig. 5. Fatigue testing machine and test specimen.**

Three different remote tensile cyclic loads (0 to 360 MPa, 0 to 375 MPa and 0 to 390 MPa) are considered to conduct high cycle fatigue tests. The fatigue lives are calculated by testing three samples for each load case. This was done in order to obtain repeatability of test findings.

## 4. Results and Discussions

The micro-hardness values measured along with the thickness and the corresponding residual stresses are discussed in the following sections.

### 4.1. Through-thickness micro-hardness results

The experimentally measured through-thickness micro-hardness in steel sheet samples derived from different coil diameter locations are shown in Fig. 6.

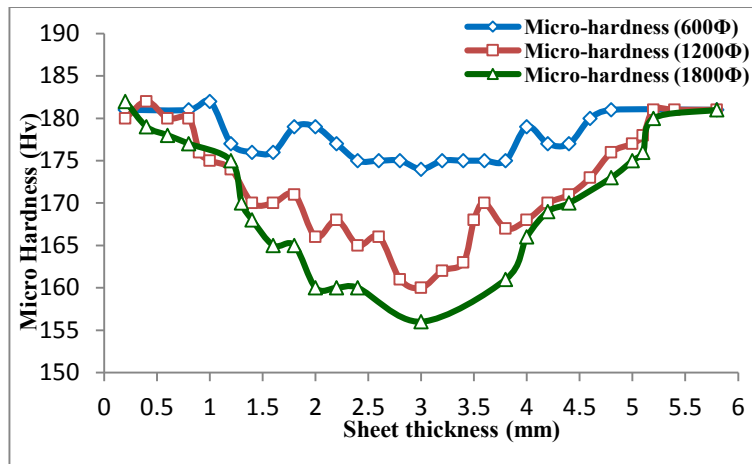


**Fig. 6. Comparison of through-thickness micro-hardness values of  $\Phi$  600 mm,  $\Phi$  1200 mm and  $\Phi$  1800 mm coil location steel samples.**

It could be observed from Fig. 6 that the Vickers micro-hardness at the core area of a steel sheet sample taken at a coil location of  $\Phi$  1800 mm has a minimum value of 156 HV. It could also be observed that at least 3 mm core thickness (from 1.25 mm to 4.25 mm thickness) of  $\Phi$  1800 mm coil sample is not affected (known as the elastic core) and the Vickers hardness values are found to be only in the range of 156 HV to 168 HV. It is only beyond the 3 mm core thickness that the steel sheet is plastically deformed and the Vickers hardness values have increased up to 182 HV.

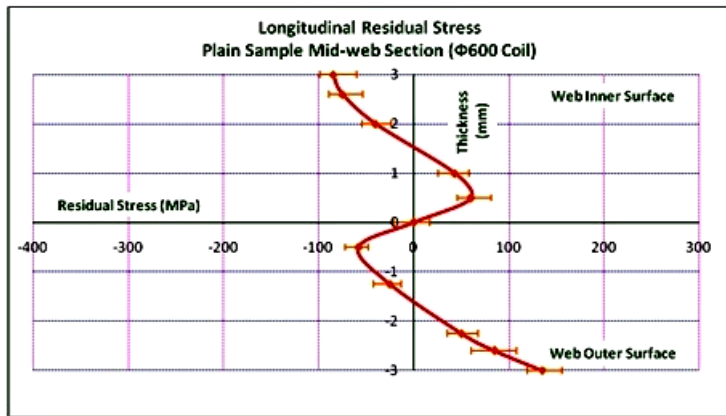
It could also be observed from Fig. 6 that the Vickers micro-hardness measured at the core area of a sample taken at a coil location of  $\Phi$  1200 mm has a minimum value of 160 HV. In this case, around 4 mm of core thickness (almost from 1 mm to 5 mm thickness) is not significantly affected by plastic deformation during the coiling-uncoiling process and the Vickers hardness values are found to be in the range of 160 HV to 175 HV. It is only beyond this 4 mm core thickness significant plastic deformation is observed and the Vickers hardness values also found to be moving towards 182 HV.

Whereas, in the sample taken at a coil location of  $\Phi$  600 mm, it is observed that almost entire steel sheet thickness is plastically deformed (although a small indistinguishable core area is observed between 2.5 mm to 3.5 mm mid-thickness area with 174 HV-175 HV) with the Vickers hardness values ranging from 174 HV to 181 HV. Residual stresses in the plastically deformed zone were measured in both longitudinal, transverse directions using Rigaku make X-ray diffractometer, and the results are discussed in the following section.

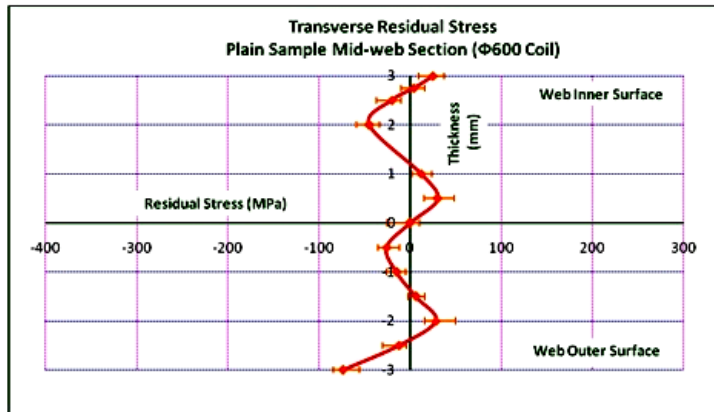
#### 4.2. Through-thickness residual stress results

As the steel strips derived from different coil diameter locations are directly used for making 'C' shaped frame rail sections, the coiling-uncoiling residual stress still remains unchanged in the plain web and flange areas of frame rail sections. Hence, it was decided to use the frame web samples taken from different coil diameter steel strips for the XRD measurement exercise.

The experimentally determined residual stresses along the thickness in the longitudinal and transverse directions of frame web samples taken from  $\Phi$  600 mm coil location are given in Figs. 7(a) and (b) respectively.



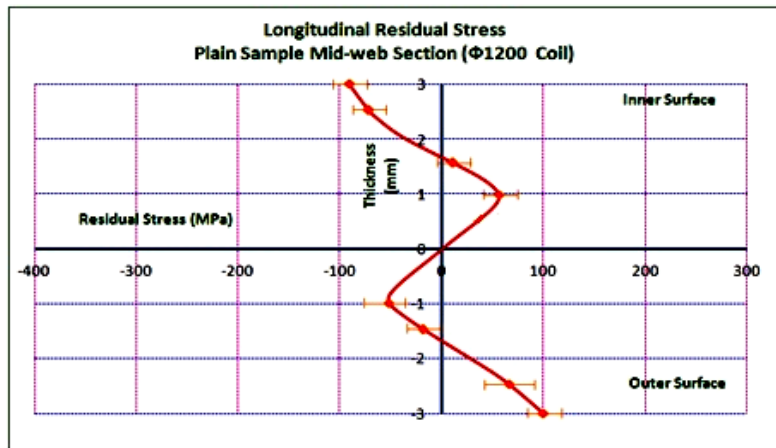
(a)



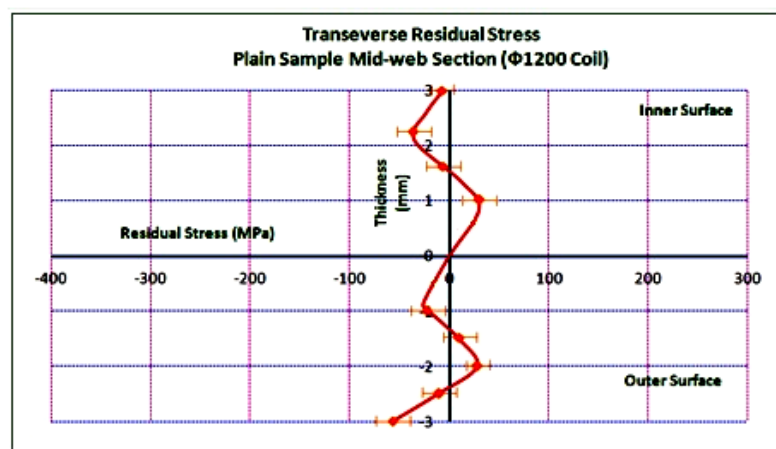
(b)

**Fig. 7(a) Longitudinal, (b) Transverse residual stresses along thickness in flat web sections taken from  $\Phi$  600 mm coil.**

The experimentally determined residual stresses along the thickness in the longitudinal and transverse directions of frame web samples taken from  $\Phi$  1200 mm coil location are given in Figs. 8(a) and (b) respectively and the experimentally determined residual stresses along the thickness in the longitudinal and transverse directions of frame web samples derived from  $\Phi$  1800 mm coil location are given in Figs. 9(a) and (b) respectively.



(a)



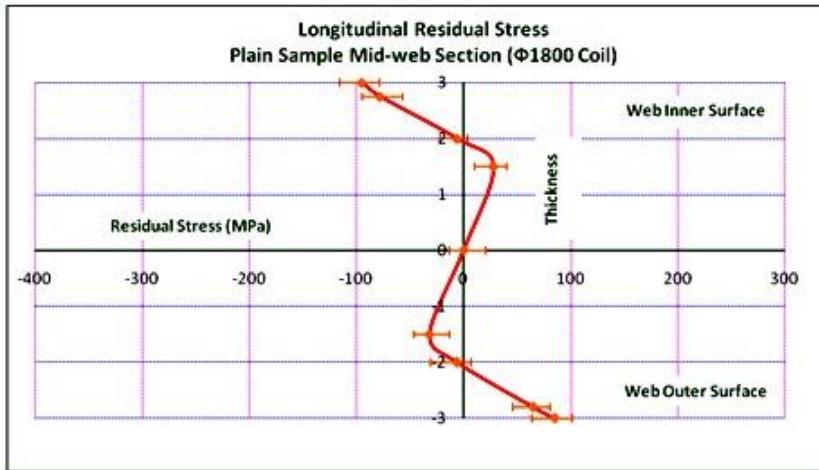
(b)

**Fig. 8(a) Longitudinal, (b) Transverse Residual stresses along thickness in flat web sections taken from  $\Phi 1200$  mm coil.**

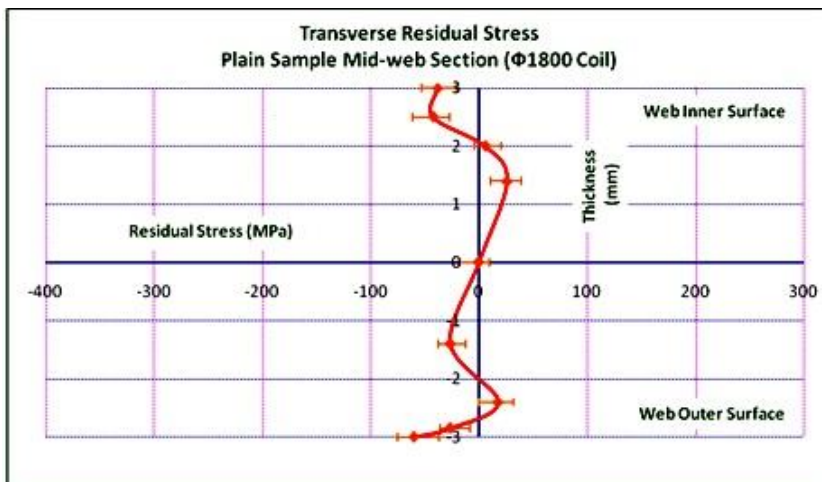
From the Figs. 7(a), 8(a) and 9(a), it could be noted that the distribution of longitudinal residual stress in plain frame web sections is non-linear. The maximum stress occurs at surfaces of the frame section. From the Figs. 7(b), 8(b) and 9(b), it is noted that the magnitudes of transverse residual stress in frame web sections are comparatively smaller and their distribution do not follow any pattern.

The magnitude of longitudinal residual stress in the frame samples taken from smaller diameter coil ( $\Phi 600$  mm) location is found to be higher than those taken from larger diameter coil ( $\Phi 1800$  mm) location. This is because smaller diameter coil location is subjected to more cold working and strain hardening during coiling-uncoiling operation than the larger diameter coil location.





(a)



(b)

**Fig. 9(a) Longitudinal, (b) Transverse residual stresses along thickness in flat web sections taken from  $\Phi 1800$  mm coil.**

Unlike corner sections of the truck frame rail, where we normally encounter tensile residual stress in the inner surface and compressive residual stress in the outer surface due to plastic bending followed by elastic spring back, in flat web and flange sections we observe the residual stress to be tensile in the outer surface and compressive in the inner surface.

This is so because of the fact that, during manufacturing of cold-formed truck frame rails, outer surface of coiled sheet (with compressive residual stress) becomes the inner surface of the frame rail web section and inner surface

of coiled sheet (with tensile residual stress) becomes outer surface of the frame rail web section respectively.

### 4.3. Elastic core depths

The unaffected elastic core depths of steel sheet during coiling-uncoiling operation are analytically calculated using the standard equation that includes the effect of Poisson ratio [11] given in Eq. (1).

$$\text{Elastic core depth} = \frac{\sigma_y(1 - \nu^2)}{EK_c(\sqrt{1 - \nu + \nu^2})} \quad (1)$$

where  $\sigma_y$  - Yield strength of steel sheet

$\nu$  - Poisson ratio

$E$  - Young's Modulus

$k_c$  - Radius of curvature of the coil.

and the calculated values of unaffected elastic core depths at different coil diameters are listed in Table 2.

**Table 2. Elastic core calculation for 6 mm steel sheet.**

Steel coil diameter (mm)	Yield strength (MPa)	Poisson ratio	Young's modulus (MPa)	Elastic core depth (mm)
600				0.97
1200	460	0.29	205000	1.94
1800				2.92

From the residual stress graphs (Figs. 6 to 8), it could be observed that the depths of unaffected elastic core during the coiling-uncoiling operation are in agreement with the analytically calculated depths of 0.97 mm, 1.94 mm and 2.92 mm for  $\Phi$  600 mm,  $\Phi$  1200 mm and  $\Phi$  1800 mm coil location respectively.

Among these residual stresses, the tensile longitudinal residual stresses prevailing in the outer web surface of frame rail (125 MPa in  $\Phi$  600 mm coil, 100 MPa in  $\Phi$  1200 mm coil and 80 MPa in  $\Phi$  1800 mm coil) will have a greater effect on the fatigue life of frame rail sections.

### 4.4. Fatigue life results

The fatigue test results of steel samples derived from three different coil diameters and annealed samples are given in Table 3 and depicted in Fig. 10.

The fatigue life of annealed flat steel samples for all three fatigue load cases is higher than the fatigue life of samples obtained from  $\Phi$  600 mm coil,  $\Phi$  1200 mm coil and  $\Phi$  1800 mm coil diameter for the corresponding fatigue load cases.

The absence of coiling-uncoiling residual stresses in annealed flat samples enhances its fatigue life.

**Table 3. Comparison of fatigue life of steel sheet samples derived from different coil diameters.**

Diameter of sample location (mm)	Stress range (MPa)	Cyclic frequency (Hz)	Fatigue life (cycles)	Coefficient of variation
600	Zero to 360	1	21541	0.286
1200			23875	0.265
1800			29158	0.207
Flat sheet (Annealed)			35804	0.232
600	Zero to 375	1	17800	0.258
1200			21542	0.137
1800			26851	0.302
Flat sheet (Annealed)			28512	0.252
600	Zero to 390	1	15100	0.114
1200			19874	0.169
1800			21651	0.243
Flat sheet (Annealed)			26547	0.176

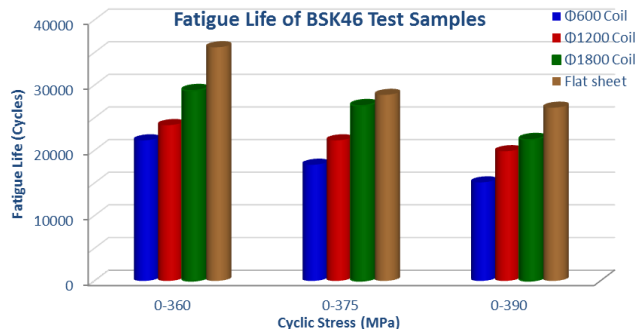


**Fig. 10. Comparison of fatigue life of steel sheet samples derived from different coil diameters.**

### 5. Conclusions

The effect of the coiling-uncoiling operation on the extent of plastic deformation, residual stress and fatigue life of steel sheets is investigated. The through-thickness plastic deformation due to coiling-uncoiling operation is first assessed with the aid of micro-hardness measurement. The through-thickness residual stress resulting from the coiling-uncoiling operation is measured by XRD and layer removal method. The overall fatigue behaviour of truck frame rail section is analysed through fatigue life experiments. From the results obtained, the following conclusions are made:

- The through-thickness micro-hardness measurements indicate the amount of plastic deformation with respect to different coil diameter location from where the specimen is taken. The extent of plastic deformation increases with the decrease in coil diameter.
- The distribution of through-thickness residual stresses in the longitudinal direction is found to be non-linear with the maximum stresses occurring at outer and inner surfaces of the web section.

- Whereas, the magnitude of residual stresses in the transverse direction of web sections are comparatively smaller and their distribution follow a complex pattern.
- The (longitudinal) tensile residual stresses prevailing in outer web surface of frame rail (125 MPa in  $\Phi$  600 mm coil, 100 MPa in  $\Phi$  1200 mm coil and 80 MPa in  $\Phi$  1800 mm coil) have a greater influence on the fatigue lives of frame rail structures.
- The fatigue lives of samples obtained from different diameter locations were found to increase with the increase in coil diameter.
- The absence of coiling-uncoiling residual stresses in annealed flat samples enhances its fatigue life.
- The fatigue life of annealed flat steel samples for all three fatigue load cases is higher than the fatigue life of samples from  $\Phi$  600 mm,  $\Phi$  1200 mm and  $\Phi$  1800 mm coil diameters.

## References

1. Quach, W.M.; Teng, J.G.; and Chung, K.F. (2004). Residual stresses in steel sheets due to coiling and uncoiling: A closed-form analytical solution. *Engineering Structures*, 26(9), 1249-1259.
2. Quach, W.M.; Teng, J.G.; and Chung, K.F. (2006). Finite element predictions of residual stresses in press-braked thin-walled steel sections. *Engineering Structures*, 28(11), 1609-1619.
3. Quach, W.M.; Teng, J.G.; and Chung, K.F. (2009). Residual stresses in press-braked stainless steel sections, i: Coiling and uncoiling of sheets. *Journal of Constructional Steel Research*, 65(8), 1803-1815.
4. Quach, W.M.; Teng, J.G.; and Chung, K.F. (2009). Residual stresses in press-braked stainless steel sections, ii: Press-braking operations. *Journal of Constructional Steel Research*, 65(8-9), 1816-1826.
5. Moen, C.D.; Igusa, T.; and Schafer, B.W. (2008). Prediction of residual stresses and strains in cold-formed steel members. *Thin-Walled Structures*, 46(11), 1274-1289.
6. Cruise, R.B.; and Gardner, L. (2008). Residual stress analysis of structural stainless steel sections. *Journal of Constructional Steel Research*, 64(3), 352-366.
7. Chinnaraj, K.; Prasad, M.S.; and Rao, C.L. (2011). Experimental analysis of residual stresses in cold formed truck frame side rail structures. *Advanced Materials Research*, 418-420, 1107-1113.
8. Chinnaraj, K.; Prasad, M.S.; and Rao, C.L. (2014). Investigation of manufacturing residual stresses in cold formed truck frame rail sections. *International Journal of Engineering Research and Applications*, 4(4), 162-169.
9. Chinnaraj, K.; Prasad, M.S.; and Rao, C.L. (2013). Numerical and experimental investigation of residual stresses in cold formed truck frame rail sections. *SAE Technical Paper*, 2013-01-2796.
10. Li, S.H.; Zeng, G.; Ma, Y.F.; Guo, Y.J.; and Lai, X.M. (2009). Residual stresses in roll-formed square hollow sections. *Thin-Walled Structures*, 47(5), 505-513.
11. Cruise, R.B. (2007). *The influence of production route on the response of structural stainless steel members*. Ph.D. Thesis. Imperial College, London.